Applied Radiation and Isotopes 129 (2017) 57–61

Contents lists available at ScienceDirect

Applied Radiation and Isotopes

journal homepage: www.elsevier.com/locate/apradiso

Automated synthesis of 1-[^{11}C]acetoacetate on a TRASIS AIO module

Kiran Kumar Solingapuram Sai[a,*], H. Donald Gage[a], Frankis Almaguel[a], Bryan Neth[b], Timothy M. Hughes[b], Sebastien Tremblay[c], Christian-Alexandre Castellano[c], Stephen C. Cunnane[c], Matthew J. Jorgensen[d], Suzanne Craft[b], Akiva Mintz[a]

[a] Department of Radiology, Wake Forest School of Medicine, Winston Salem, NC, USA
[b] Department of Internal Medicine, Wake Forest School of Medicine, Winston Salem, NC, USA
[c] Research Center on Aging, Sherbrooke Molecular Imaging Center, Université de Sherbrooke, Sherbrooke, Quebec, Canada
[d] Department of Pathology-Comparative Medicine, Wake Forest School of Medicine, USA

HIGHLIGHTS

- Automated and simplified production of 1-[^{11}C]acetoacetate using TRASIS AIO module.
- 1-[^{11}C]acetoacetate radiochemistry can be directly translated and easily adapted to any automated modules for human injections.
- 1-[^{11}C]acetoacetate production was validated through monkey PET imaging studies for the first time.

ARTICLE INFO

Keywords:
Automation
Ketone metabolism
PET imaging
Ion-exchange column
Formulations
Non-Human primates

ABSTRACT

We automated radiochemical synthesis of 1-[^{11}C]acetoacetate in a commercially available radiochemistry module, TRASIS AllInOne by [^{11}C]carboxylation of the corresponding enolate anion generated *in situ* from isopropenylacetate and MeLi, and purified by ion-exchange column resins.1-[^{11}C]acetoacetate was synthesized with high radiochemical purity (95%) and specific activity (~ 66.6 GBq/μmol, n = 30) with 35% radiochemical yield, decay corrected to end of synthesis. The total synthesis required ~ 16 min. PET imaging studies were conducted with 1-[^{11}C]acetoacetate in vervet monkeys to validate the radiochemical synthesis. Tissue uptake distribution was similar to that reported in humans.

1. Introduction

Under normal conditions, glucose is the brain's primary fuel; however during prolonged fasting or at lower plasma glucose concentrations, fat-derived ketones constitute the brain's main fuel (Cunnane et al., 2016; Willis et al., 2002). Ketone bodies consist of acetoacetate, *β*-hydroxybutyrate and acetone. These play a vital role in brain lipid synthesis in the fetus and in infant brain development (Roy et al., 2012; Yudkoff et al., 2004). During long-term starvation in adults, plasma ketones reach a concentration of 2–6 mM and can supply up to ~ 70% of the brain's fuel needs (Bianchi and Davis, 1996; Owen et al., 1967).

Alzheimer's disease (AD) is the most common neurodegenerative disease and the leading cause of severe dementia, especially among the older adults. The occurrence of AD exponentially increases with age once individuals reach 65 years of age or older. There is no specific treatment regimen to preclude the symptoms of AD nor are the presently available ones are effective. Low uptake of 2-[^{18}F]fluoro-D-glucose ([^{18}F]FDG) in AD-susceptible regions has been proposed as a key markers in AD pathophysiology (Mosconi, 2005). Considerable scientific evidence suggests that brain glucose metabolism is inhibited during AD (Bianchi and Davis, 1996; Castellano et al., 2015). As the main fuel alternate to glucose, ketones can account for up to 60% of brain metabolic demands in order to help mitigate states of decreased glucose metabolism in AD. One of the ketone-based strategies studies aimed at slowing the progression of AD in the high Fat-ketogenic diet. One of the several research pathways studied to improve the conditions of AD is 'ketogenic diet"(Cunnane et al., 2010; Elwood et al., 1960; Loessner et al., 1995; Owen et al., 1967; Pifferi et al., 2008). Cognitive function can be significantly improved in memory-impaired adults by a ketogenic diet intervention (Courchesne-Loyer et al., 2012; Krikorian et al., 2010; Nugent et al., 2014; Pifferi et al., 2008; Yudkoff et al., 2004).

Current strategies to assess brain metabolism using [^{18}F]FDG provide no information regarding the brain's innate ability to use ketone

Abbreviations: [^{11}C]AcAc, 1-[^{11}C]acetoacetate; FDG, 2-[^{18}F]fluoro-D-glucose; PET, Positron Emission Tomography; NHP, Non-Human Primate; EOS, End Of Synthesis

* Corresponding author.
E-mail address: ksolinga@wakehealth.edu (K.K. Solingapuram Sai).

http://dx.doi.org/10.1016/j.apradiso.2017.07.066
Received 17 December 2016; Received in revised form 24 May 2017; Accepted 31 July 2017
Available online 02 August 2017
0969-8043/

bodies. PET imaging using [^{11}C]acetoacetate ([^{11}C]**AcAc**) can provide quantitative analysis of brain ketone utilization that can help uncover the role of ketone metabolism in early AD; such information could potentially lead to new preventive and therapeutic strategies (Authier et al., 2008; Courchesne-Loyer et al., 2016; Nugent et al., 2013). These promising translational imaging applications of [^{11}C]**AcAc** stimulated efforts for the development of a more robust and simple automated radiochemistry procedure. While previous investigators have automated [^{11}C]**AcAc** synthesis in a custom-built radiochemistry module (Tremblay et al., 2007), simplifying this production in a more commercially available automated unit will pave the path for widespread use of the radiopharmaceutical in clinical settings. TRASIS AIO is an automated, commercially available radiosynthesis module that produces GMP grade PET radiopharmaceuticals for human injections and is being widely used in several PET centers across the world. Here, we report for the automated synthesis [^{11}C]**AcAc** in TRASIS AllInOne module and report its utility in non-human primates (NHP).

2. Materials and methods

The following chemical reagents were purchased from Sigma-Aldrich (St. Louis, MO) and were used without any additional purification: methyllithium (MeLi, 1.6 M diethylether), isopropenylacetate (IPA), anhydrous tetrahydrofuran (THF), sodium hydroxide solution (NaOH, 1.0 M), citric acid monohydrate (CAM), trisodium citric acid (TCA), sodium chloride (NaCl) and lithium acetoacetate (LAA). All reactions were carried out using anhydrous solvents unless otherwise stated. Both the resin materials *i.e.,* Dowex × 8–100 (cation resin material) and AG 1X-8 (anion exchange resin material), chromatography flex columns and the analytical HPLC column heater were purchased from Fisher Scientific (Hampton, NH). Aqueous 5 mM sulfuric acid (H_2SO_4) solution was purchased from VWR scientific (Radnor, PA). Analytical HPLC was performed using Varain ProStar system, which includes quaternary gradient pump, manual injector, a variable wavelength detector and a standard Bioscan radioactivity-HPLC-flow detector. Aminex HPX-87 H analytical column (300 × 70 mm) was purchased from BIO-RAD (Hercules, CA). Sterile pyrogen-free filters were purchased from Millipore Corp (Billerica, MA).

2.1. TRASIS AIO preparation

TRASIS AllInOne (AIO) is a commonly used radiochemistry module for clinical GMP-grade radiopharmaceutical production (AIO, 2014). [^{11}C]**AcAc** radiosynthesis was carried out with TRASIS AIO module using the ports as shown in Fig. 1.

2.2. Cartridge conditioning and citrate buffer setup

Citrate buffer solution, pH 4.0 for eluting the final radioactive product [^{11}C]**AcAc** was made according to the previously published procedures (Tremblay et al., 2007). Briefly, for a stock solution (25 mL), CAM (0.3 g, 1.42 mM), TCA (0.18 g, 0.7 mM) and NaCl (0.12 g, 1.95 mM) were added in a sterile laminar fume hood. The solution was stored at 4 °C and was filtered through a 0.22 μm pyrogen-free Millipore filter for every batch synthesis. Both the cation and anion exchange resin cartridges were pre-conditioned following published procedures. Briefly, Dowex 50WX8-100 was placed in a small chromatography flex column and washed with sterile water (10 mL). AG 1X-8 was placed in a separate flex column and washed with aqueous NaOH solution (5 mL, 1.0 M) followed by sterile water (25 mL). Both the ion exchange resin materials had a final pH between 7.0 and 7.5

2.3. Radiochemical synthesis of [^{11}C]*AcAc*

2.3.1. Production of [^{11}C]CO_2

[^{11}C]CO_2 was produced in the Wake Forest PET Center cyclotron facility on a GE PETtrace- 800 cyclotron. [^{11}C]CO_2 was produced from the nuclear reaction $^{14}N(p,\alpha)^{11}C$ by proton bombardment of a niobium target to a pressure of 17.2 bar (250 psi). A nitrogen target containing 0.2% oxygen was irradiated for 15–20 min with a 45 μA beam of 16 MeV protons, to produce up to 40–42 GBq of [^{11}C]CO_2 (Solingapuram et al., 2014). [^{11}C]CO_2 released from the GE PET-trace cyclotron was directly bubbled and trapped into the reaction vial assembled in the TRASIS AIO module using anhydrous potassium perchlorate ($KClO_4$, 8 g) trap.

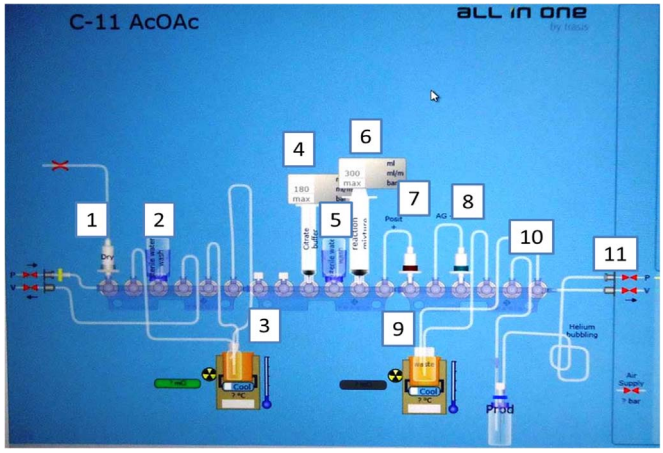

Fig. 1. TRASIS AIO reaction program screenshot for [^{11}C]**AcAc** radiosynthesis. Port#1 [^{11}C]CO_2; Port #2 sterile water setup-hydrolysis; Port #3 reaction vial holder 1; Port# 4 citrate buffer solution (10 mL syringe) 5 mL, pH 4.0; Port#5 sterile water setup-washing AG 1X-8 cartridge; Port#6 reaction mixture syringe (20 mL syringe); Port #7 cartridge holder for Dowex × 8–100 (cation exchange resin material); Port#8 cartridge holder for AG 1X-8 (anion exchange resin material); Port#9 reaction vial holder 2 (waste vial); Port#10 product line; Port #11 helium degassing line.

2.3.2. Precursor reaction mixture setup

The enolate anion of acetone was prepared following a previously published method with slight modification (Tremblay et al., 2008, 2007). Briefly, IPA (1.0 eq) was slowly added drop-wise to the glass vial loaded with MeLi (1.6 M in diethyl ether, 1.85 eq) at − 75 °C under inert conditions. Anhydrous THF (0.75 mL) was slowly added to the reaction mixture and allowed to stir for 1 h at − 40 °C to − 70 °C under an inert atmosphere (Scheme 1). MeLi afforded better yields of final radioactive product when used as a base, compared to *n*BuLi. The crude enolate solution formed *in situ* was used for radiolabeling as is without any additional purification.

2.3.3. [^{11}C]*AcAc* production

Optimized radiosynthesis of [^{11}C]**AcAc** was completed *via* carboxylation, hydrolysis, resin cartridge purification and citrate buffer formulation (Tremblay et al., 2007). The TRASIS AIO setup for radiosynthesis is shown in Fig. 2. Firstly, the crude enolate solution (0.8–1.3 mL) synthesized from MeLi-base catalyzed reaction of isopropenylacetate was placed in the reaction vial holder#1of the TRASIS AIO module, once the module was ready to receive [^{11}C]CO_2 gas from the cyclotron. The vial was then cooled to − 10 °C to − 40 °C using liquid nitrogen cooling setup from the module. [^{11}C]CO_2 released from the cyclotron was bubbled and trapped into the reaction vial with the enolate solution at the same temperature. After complete transfer of radioactivity (3–4 min), the radioactive reaction mixture was allowed

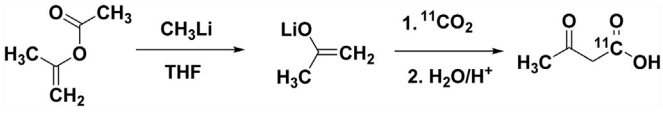

Scheme 1. Radiosynthesis of [^{11}C]**AcAc**.

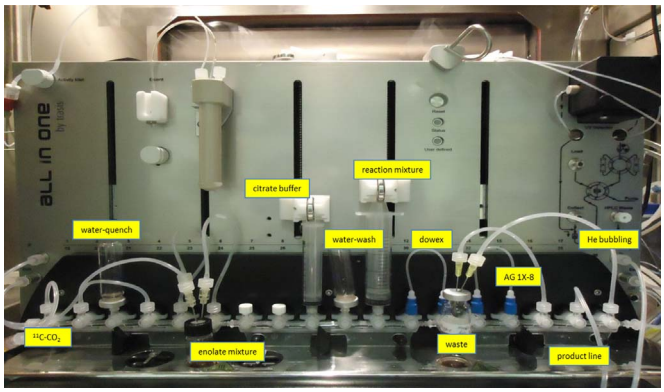

Fig. 2. TRASIS AIO reaction setup for [^{11}C]**AcAc** radiosynthesis.

to react for an additional 6 min, which brought the vial temperature to 5–10 °C. The reaction mixture was then hydrolyzed with sterile water (10 mL), drawn into the 20 mL syringe using helium, and then pushed back into the vial for thorough mixing. From the 20 mL syringe, the reaction mixture solution was slowly pushed through the (+)Dowex and (−)AG 1X-8 resin cartridges into the waste vial (placed in reaction vial holder #2). At this step, the desired product [^{11}C]**AcAc** was trapped in AG 1X-8 cartridge. To remove undesired water soluble impurities, the AG 1X-8 cartridge was washed with an additional 10 mL of sterile water that passed into the waste vial, the cartridge was allowed to dry using helium flow for 1.5 min. The radioactive product [^{11}C]**AcAc** was eluted from the AG 1X-8 cartridge with citrate buffer solution (pH = 4.0), coming from port # 4 from a 10 mL syringe. The final product was directly eluted into the final product vial through a sterile 0.22 μm pyrogen-free Millipore filter. The final product vial with [^{11}C]**AcAc** was then degassed using helium for an additional 1.5 min to remove any excess [^{11}C]CO_2 and was used for quality control analysis and animal studies.

The chemical and radiochemical purity of the collected radioactive aliquot was checked by performing a HPLC injection on an Aminex HPX-87 H analytical column (300 × 70 mm) at 35 °C using a column heater. The mobile phase was aqueous sulfuric acid solution (aq. H_2SO_4, 5 mM) and the UV detection was set at 210 nm with a flow rate of 0.75 mL/min. Under these conditions, the single injection of [^{11}C]**AcAc** had a retention time of 13.1 min. The radioactive peak was further authenticated by performing a co-injection with the standard lithium acetoacetate, which displayed a similar retention time.

2.4. Monkey PET imaging studies

All animal experiments were conducted under IACUC approved protocols in compliance with the guidelines for the care and use of research animals established by Wake Forest Medical School Animal Studies Committee. PET imaging studies of [^{11}C]**AcAc** were performed in adult female vervet monkeys (n = 10, ~ 4–7 kg) between 8 and 23 y old. We used a GE 16-slice PET/CT Discovery ST Scanner with 24 detector rings that provide 47 contiguous image planes over a maximum 70 cm transaxial field of view with CT attenuation correction. Monkeys were fasted for 12 h before the PET study. The animals were initially anesthetized using intramuscular ketamine (10 mg/kg) and transported to the PET scanner suite. Upon arrival, each monkey was intubated with an endotracheal tube and anesthesia was maintained at 1.5% isoflurane/oxygen throughout the PET scanning procedure. The monkey was placed in the scanner and a catheter inserted into an external vein for tracer injection and fluid replacement. Body temperature was maintained at 40 °C and vital signs (heart rate, blood pressure, respiration rate, and temperature) monitored throughout the scanning procedure.

An initial low-dose CT-based attenuation correction scan was acquired. Next, [^{11}C]**AcAc** (0.18 – 0.3 GBq) was injected and a 30-min dynamic whole body acquisition scan was acquired. 70 frames were acquired over 30 min (6 × 10 s, 15 × 120 s) in 3D mode (*i.e.,* septa retracted). For each frame, image reconstruction of the acquired emission data was done with full quantitative corrections including attenuation and reconstructed into forty-seven 128 × 128 matrices (Bentourkia et al., 2009; Nugent et al., 2013). Data was analyzed using PMOD Biomedical Image Quantification Software (version 3.5; PMOD Technologies, Zurich, Switzerland). Uptake in the brain and other organs (including lung, liver, spleen, kidney, heart and muscle) were defined by its standardized uptake value (SUV) calculated by dividing the tracer concentration in each pixel by the injected dose per body mass. On the dynamic scan, regions of interests were drawn on the whole brain and time activity curves were generated.

3. Results and discussion

3.1. Radiochemistry

[^{11}C]**AcAc** radiosynthesis was first developed by Tremblay et al. in a custom-built C-11 radiochemistry module with vials and pressure/vacuum gauge setups for gas flow (Tremblay et al., 2007). We simplified and automated radiosynthesis in a commercially available radiochemistry device, the TRASIS AIO. Previous approaches employed drying methods ranging from molecular sieves with a helium conditioning setup to dry incoming radioactive [^{11}C]CO_2 gas from the cyclotron (Prenen et al., 1990; Tremblay et al., 2008, 2007). We have simplified the entire drying process by using a $KClO_4$ trap. This $KClO_4$ trap was changed once for every 20–25 syntheses.

Radiolabeling of [^{11}C]**AcAc** was accomplished by employing simple and convenient conditions for C-11 carboxylation of the enolate anion of acetone, generated *insitu* from the MeLi-catalyzed reaction of IPA in THF. Carboxylation, hydrolysis, ion-exchange resin purification and formulation as outlined in Fig. 2 resulted in [^{11}C]**AcAc** processed in the TRASIS AIO module with ~ 35% radiochemical yield after final formulation including degassing. The radiochemical purity of [^{11}C]**AcAc** was greater than 95% and chemical purity was great than 90%. [^{11}C]**AcAc** was identified by co-eluting with a solution of standard lithium acetoacetate. Retention time of [^{11}C]**AcAc** on the analytical HPLC system was 13.1 −13.5 min. Apart from the acetoacetate peak, trace peaks of sodium chloride at 5.8 min citrate buffer 7.6 min and carbonic acid at 17 min were obtained in the UV chromatogram. [^{11}C]**AcAc** was obtained in a specific activity of ~ 66.6 GBq/μmol (decay corrected to EOS, n = 30), which is sufficient for *in vivo* validation. The entire synthetic procedure, including production of [^{11}C]CO_2 trapping, reaction, resin purification and formulation of the radiotracer for *in vivo* studies, was completed within 16 min. Due to the simplification and automation of the process, the radiochemical synthesis of [^{11}C]**AcAc** can be easily translated to other automated radiochemistry modules.

3.2. Monkey PET image analysis

To validate the automated synthesis of [^{11}C]**AcAc**, dynamic whole-body PET imaging was performed in female vervet monkeys (n = 6). 30 min post-injection, tissue uptake was captured as SUV based radioactive organ distribution (Fig. 3). [^{11}C]**AcAc** time-activity curves from the whole brain regions of monkeys (n = 2), as demonstrated in Fig. 4, showed the anticipated wash-out kinetics for a typical C-11 PET radiopharmaceutical to be adapted for clinical settings (Harapanhalli, 2010).

The radioactive uptake, kinetics and distribution pattern of [^{11}C]**AcAc** in monkey brain (through PET imaging) were very similar to those pattern observed in human brain (Nugent et al., 2013). [^{11}C]**AcAc** readily entered the brain and peaks within 5 min of injection (Neth B, 2016). The organ distribution of [^{11}C]**AcAc**, shown in Fig. 3

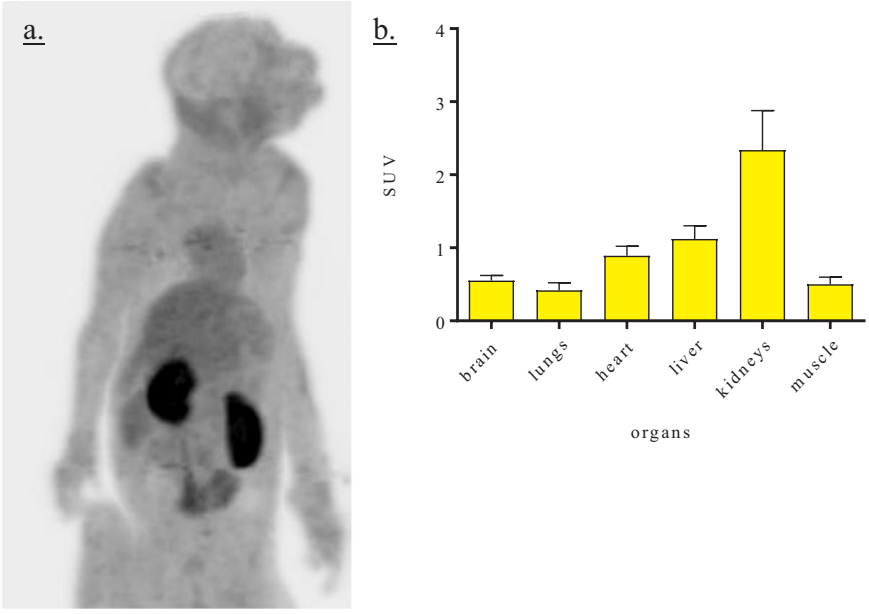

Fig. 3. a. Whole body PET image b. organ biodistribution through PET- SUV data analysis (n = 6) of adult vervet monkey obtained after *iv* injection of [^{11}C]**AcAc** (0.3 GBq).

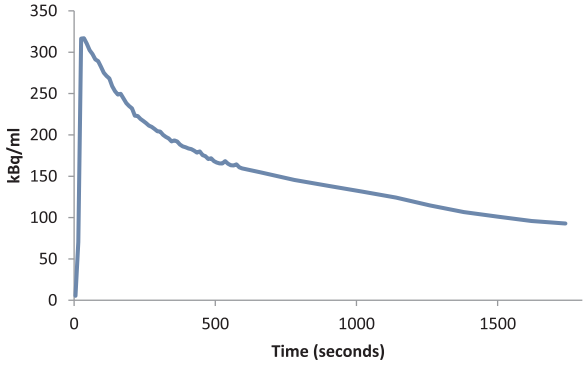

Fig. 4. Representative time activity curves (TACs) starting from 0 to 1800 s from a female monkey whole brain injected with [^{11}C]**AcAc** (0.3 GBq).

demonstrated predominant renal clearance with notable uptake in the heart and liver. This is significant due to the interest in using [^{11}C]**AcAc** imaging for cardiovascular studies in nonhuman primates, since it is a substrate of cardiac metabolism (Croteau et al., 2010, 2014; Maalouf and Yin, 2013).

4. Conclusions

We report the simplified and automated radiolabeling procedure for [^{11}C]**AcAc** with high radiochemical yield, radiochemical purity and specific activity. This method can be directly translated and easily adapted to any automated modules for human injections and clinical trials. We further validated the radioactive uptakes of [^{11}C]**AcAc** in vervet monkeys using PET imaging studies for the first time. The radioactive uptake, distribution and clearance patterns of [^{11}C]**AcAc** were similar to those in humans, raising the possibility of using these methods to explore alternate brain energy metabolism in nonhuman primate models of human diseases. This study strongly reinforces the utility of [^{11}C]**AcAc** PET studies to uncover the role of ketone metabolism in normal and disease states, and could lead to new preventive and therapeutic strategies. In particular, translational [^{11}C]**AcAc** PET imaging studies might fill the missing gaps in understanding early features of AD and its progression to dementia, using ketogenic diet interventions.

Funding sources

This work was supported by charitable donations from the Hartman Foundation, the NIH 1R01CA179072 (Mintz), an American Cancer Society Mentored Research Scholar grant 124443-MRSG-13-121-01-CDD (Mintz), the NIH Vervet Research Colony grant (P40-OD010965), the NIH AD Center grant (P30AG049638) and the Translational Imaging and Wake Forest Translational Imaging Program – Clinical Translational Science Institute (UL1TR001420) and the Université de Sherbrooke Research Chair in Brain Metabolism and Aging.

References

AIO, T., 2014. TRASIS AllinOne GMP Universal Radiosynthesis Unit, ⟨http://www.trasis.com/pages/all_in_one.html⟩, p. TRASIS automated instrument.

Authier, S., Tremblay, S., Dumulon, V., Dubuc, C., Ouellet, R., Lecomte, R., Cunnane, S.C., Benard, F., 2008. [^{11}C] acetoacetate utilization by breast and prostate tumors: a PET and biodistribution study in mice. Mol. Imaging Biol. 10, 217–223.

Bentourkia, Mh, Tremblay, S., Pifferi, F., Rousseau, J., Lecomte, R., Cunnane, S., 2009. PET study of [^{11}C]-acetoacetate kinetics in rat brain during dietary treatments affecting ketosis. Am. J. Physiol. – Endocrinol. Metab. 296, E796–E801.

Bianchi, P.B., Davis, A.T., 1996. β-hydroxybutyrate oxidation is reduced and hepatic balance of ketone bodies and free fatty acids is unaltered in carnitine-depleted, pivalate-treated rats. J. Nutr. 126, 2867–2872.

Castellano, C.-A., Nugent, S., Paquet, N., Tremblay, S., Bocti, C., Lacombe, G., Imbeault, H., Turcotte, E., Fulop, T., Cunnane, S.C., 2015. Lower brain ^{18}F-fluorodeoxyglucose uptake but normal ^{11}C-acetoacetate metabolism in mild Alzheimer's disease dementia. J. Alzheimer's Dis. 43, 1343–1353.

Courchesne-Loyer, A., Croteau, E., Castellano, C.-A., St-Pierre, V., Hennebelle, M., Cunnane, S.C., 2016. Inverse relationship between brain glucose and ketone metabolism in adults during short-term moderate dietary ketosis: a dual tracer quantitative positron emission tomography study. J. Cereb. Blood Flow. Metab.

Courchesne-Loyer, A., Fortier, M., Tremblay-Mercier, J., Chouinard-Watkins, R., Roy, M., Nugent, S., Castellano, C.-A., Cunnane, S.C., 2012. Stimulation of mild, sustained ketonemia by medium-chain triacylglycerols in healthy humans: estimated potential contribution to brain energy metabolism. Nutrition 29, 635–640.

Croteau, E., Tremblay, S., Dumulon-Perreault, V., Cunnane, S., Langlois, R., Lecomte, R., Benard, F., 2010. 11C-acetoacetate as a PET cardiac imaging agent of cardiotoxicity. J. Nucl. Med. 51, 264.

Croteau, E., Tremblay, S., Gascon, S., Dumulon-Perreault, V., Labbé, S.M., Rousseau, J.A., Cunnane, S.C., Carpentier, A.C., Bénard, F., Lecomte, R., 2014. [11C]-Acetoacetate PET imaging: a potential early marker for cardiac heart failure. Nucl. Med. Biol. 41, 863–870.

Cunnane, S., Nugent, S., Roy, M., Courchesne-Loyer, A., Croteau, E., Tremblay, S., Castellano, A., Pifferi, F., Bocti, C., Paquet, N., Begdouri, H., Bentourkia, Mh, Turcotte, E., Allard, M., Barberger-Gateau, P., Fulop, T., Rapoport, S.I., 2010. Brain fuel metabolism, aging, and Alzheimer's disease. Nutrition 27, 3–20.

Cunnane, S.C., Courchesne-Loyer, A., Vandenberghe, C., St-Pierre, V., Fortier, M., Hennebelle, M., Croteau, E., Bocti, C., Fulop, T., Castellano, C.-A., 2016. Can ketones help rescue brain fuel supply in later life? Implications for cognitive health during aging and the treatment of Alzheimer's disease. Front. Mol. Neurosci. 9.

Elwood, J.C., MarcÃ³, A., Van Bruggen, J.T., 1960. Lipid metabolism in the diabetic rat: IV. Metabolism of acetate, acetoacetate, butyrate, and mevalonate in vitro. J. Biol. Chem. 235, 573–577.

Harapanhalli, R.S., 2010. Food and drug administration requirements for testing and approval of new radiopharmaceuticals. Semin. Nucl. Med. 40, 364–384.

Krikorian, R., Shidler, M.D., Dangelo, K., Couch, S.C., Benoit, S.C., Clegg, D.J., 2010. Dietary ketosis enhances memory in mild cognitive impairment. Neurobiol. Aging 33, 425.e419–425.e427.

Loessner, A., Alavi, A., Lewandrowski, K.-U., Mozley, D., Souder, E., Gur, R.E., 1995. Regional cerebral function determined by FDG-PET in healthy volunteers: normal patterns and changes with age. J. Nucl. Med. 36, 1141–1149.

Maalouf, M., Yin, J., 2013. Abstract TP126: the ketones acetoacetate and beta-hydroxybutyrate alleviate ischemic injury following occlusion of the middle cerebral artery. Stroke 44 (ATP126-ATP126).

Mosconi, L., 2005. Brain glucose metabolism in the early and specific diagnosis of Alzheimer's disease. Eur. J. Nucl. Med. Mol. Imaging 32, 486–510.

Neth B, M.A., Solingapuram Sai, K.K, Gage, D., Shively, C., Register, T., Jorgenson, M., Andrews. R., Atkins. H., Uberseder. B., Cline. J.M., Cunnane. S., Castellano. C., Keene. D., Montine. T., Maldjian. J., Wagner. B., Hughes. T., Craft, S., 2016. Dual-tracer acetoacetate and glucose metabolism are associated with neuropathologic amyloid burden and Alzheimer's biomarkers in the CSF. In: Proceedings of the Alzheimer's Association International Conference 2016. Alzheimer's & Dementia: The Journal of the Alzheimer's Association, Toronto, ON, Canada. July 2016.

Nugent, S., Castellano, C.-A., Goffaux, P., Whittingstall, K., Lepage, M., Paquet, N., Bocti, C., Fulop, T., Cunnane, S.C., 2014. Glucose hypometabolism is highly localized but lower cortical thickness and brain atrophy are widespread in cognitively normal older adults. Am. J. Physiol. – Endocrinol. Metab.

Nugent, S., Tremblay, S., Chen, K.W., Ayutyanont, N., Roontiva, A., Castellano, C.-A., Fortier, M., Roy, M., Courchesne-Loyer, A., Bocti, C., Lepage, M., Turcotte, E., Fulop, T., Reiman, E.M., Cunnane, S.C., 2013. Brain glucose and acetoacetate metabolism: a comparison of young and older adults. Neurobiol. Aging 35, 1386–1395.

Owen, O.E., Morgan, A.P., Kemp, H.G., Sullivan, J.M., Herrera, M.G., Cahill, G.F., 1967. Brain metabolism during fasting. J. Clin. Investig. 46, 1589–1595.

Pifferi, F., Tremblay, S., Plourde, M., Tremblay-Mercier, J., Bentourkia, Mh, Cunnane, S.C., 2008. Ketones and brain function: possible link to polyunsaturated fatty acids and availability of a new brain PET tracer, ^{11}C-acetoacetate. Epilepsia 49, 76–79.

Prenen, G.H.M., Go, K.G., Zuiderveen, F., Paans, A.M.J., Vaalburg, W., 1990. An improved synthesis of carbon-11 labeled acetoacetic acid and an evaluation of its potential for the investigation of cerebral pathology by positron emission tomography. Int. J. Radiat. Appl. Instrum. Part A. Appl. Radiat. Isot. 41, 1209–1216.

Roy, M., Nugent, S., Tremblay-Mercier, J., Tremblay, S., Courchesne-Loyer, A., Beaudoin, J.-F., Tremblay, L., Descoteaux, M., Lecomte, R., Cunnane, S.C., 2012. The ketogenic diet increases brain glucose and ketone uptake in aged rats: a dual tracer PET and volumetric MRI study. Brain Res. 1488, 14–23.

Solingapuram, K.K., Fan, J., Tu, Z., Zerkel, P., Mach, R.H., Kharasch, E.D., 2014. Automated radiochemical synthesis and biodistribution of [(11)C]l-Î ± -acetylmethadol ([(11)C]LAAM). Appl. Radiat. Isot.: Incl. data Instrum. Methods Use Agric. Ind. Med. 91, 135–140.

Tremblay, S., Ouellet, R., Bénard, F., Cunnane, S.C., 2008. Automated synthesis of ^{11}C-β-hydroxybutyrate by enzymatic conversion of ^{11}C-acetoacetate using β-hydroxybutyrate dehydrogenase. J. Label. Compd. Radiopharm. 51, 242–245.

Tremblay, S., Ouellet, R., Rodrigue, S., Langlois, R., Benard, F., Cunnane, S.C., 2007. Automated synthesis of ^{11}C-acetoacetic acid, a key alternate brain fuel to glucose. Appl. Radiat. Isot. 65, 934–940.

Willis, M.W., Ketter, T.A., Kimbrell, T.A., George, M.S., Herscovitch, P., Danielson, A.L., Benson, B.E., Post, R.M., 2002. Age, sex and laterality effects on cerebral glucose metabolism in healthy adults. Psychiatry Res.: Neuroimaging 114, 23–37.

Yudkoff, M., Daikhin, Y., Nissim, I., Lazarow, A., Nissim, I., 2004. Ketogenic diet, brain glutamate metabolism and seizure control. Prostaglandins, Leukot. Essent. Fat. Acids 70, 277–285.